Nuclear kinetic energy spectra of D_2^+ in an intense laser field: Beyond the Born-Oppenheimer approximation

Mohsen Vafaee*
Department of Chemistry, University of Isfahan, Isfahan 81746-73441, Iran
(Received 12 November 2007; published 19 August 2008)

Simultaneously, the vibrational nuclear dynamics and full dimensional electronic dynamics of a deuterium molecular ion exposed to a linear polarized intense laser field are studied. The time-dependent Schrödinger equation of an aligned D_2^+ ion with electric laser field is solved for a simulation of complicated dissociative ionization processes and compared with recent related experimental results. We introduce and calculate the *R*-dependent ionization rate and the enhanced ionization phenomenon beyond the Born-Oppenheimer approximation. The substructure of the nuclear kinetic energy release spectra is revealed as the Coulomb explosion energy spectra and dissociation energy spectra in the dissociation-ionization channel. The significance and trace of these distinct subspectra in the total spectra are comparatively displayed and discussed.

DOI: 10.1103/PhysRevA.78.023410 PACS number(s): 33.80.Rv, 33.80.Gj, 42.50.Hz

INTRODUCTION

H_2 and H_2^+, two basic molecules, have been extensively studied experimentally and theoretically. These studies have uncovered comprehensive new phenomena [1]. Studies of the dynamics of H_2 (D_2) and H_2^+ (D_2^+) exposed to an intense laser field are very complicated because of involved two processes involved: ionization and dissociation simultaneously. In an intense laser field, electron dynamics occurs in attosecond time scales and nuclear dynamics, vibration and rotation, takes place in femtosecond and picosecond time scales. It is possible based on the Born-Oppenheimer approximation (BOA) to investigate these two dynamics, nuclear and electronic, separately. This approach has been extensively used to investigate the electronic dynamics of molecules in intense laser fields. When a molecule is exposed to an intense laser field, an accurate probe of the molecular dynamics that is involved simultaneously, electronic and nuclear dynamics is very complicated. In these conditions, the perfect complicated simulation based on a solution of the time-dependent Schrödinger equation (TDSE) beyond the BOA, the most rigorous and adequate, *ab initio* theoretical approach, would require one to a complete description of molecular dynamics. For a molecule with two or more electrons, this task is very far from present available computer abilities, even without consideration of the nuclear dynamics [2]. For a linear molecule with only one electron, this rigorous approach is feasible only for an aligned molecule with the electric laser field together with a reduction of the dimensions of the electronic motion. Therefore, most theoretical investigations have been carried out for dissociative ionization of aligned H_2^+ (D_2^+) parallel to the electric field axis of a linear polarized laser pulse, and three spatial coordinates of the electron in the TDSE are reduced to one dimension (1D) based in an approximation known as the quasi-Coulombic or soft-core (SC) Coulomb potential [3] to be able to carry out simulations, so that much research was done based on the SC approximation [4–7] even for two-electron systems [8]. Nevertheless, the extent of the ability and validity of the SC approximation in research on electron dynamics in multielectron systems especially involving one and two electrons has been the subject of controversy. The results of this work will explore this question. In this research, the previous studies are extended. We have done perfect complicated simulations of D_2^+ beyond the BOA and also without the SC approximation—i.e., by the rigorous solution of the TDSE for the full dimensional electron dynamics and also with consideration of the nuclear dynamics of D_2^+ that is aligned with the electric laser field.

NUMERICAL SOLUTION OF THE TDSE AND DISCUSSION

The time-dependent Schrödinger equation in the cylindrical polar coordinate system for H_2^+ (D_2^+) located in the laser field as $E(t)=E_0 f(t)\cos(\omega t)$ parallel to the internuclear axis in atomic units ($\hbar=m_e=e=1$) reads as (throughout of this article we use the atomic unit unless stated)

$$i\frac{\partial\psi(z,\rho,R,t)}{\partial t}=H(z,\rho,R,t)\psi(z,\rho,R,t), \tag{1}$$

where the total 3D electronic Hamiltonian is given by [9–11]

$$H(z,\rho,R,t)=-\frac{2m_N+m_e}{4m_N m_e}\left[\frac{\partial^2}{\partial\rho^2}+\frac{1}{\rho}\frac{\partial}{\partial\rho}+\frac{\partial^2}{\partial z^2}\right]-\frac{1}{m_N}\frac{\partial^2}{\partial R^2}+V_C(z,\rho,R,t), \tag{2}$$

$$V_C(z,\rho,R,t)=\frac{-1}{\sqrt{(z+R/2)^2+\rho^2}}+\frac{-1}{\sqrt{(z-R/2)^2+\rho^2}}+\frac{1}{R}+\left(\frac{2m_p+2m_e}{2m_p+m_e}\right)zE_0 f(t)\cos(\omega t), \tag{3}$$

with E_0 being the laser peak amplitude, $\omega=2\pi\upsilon$ the angular frequency, and finally $f(t)$ the laser pulse envelope, which is set as

*Mohsenvafaee@gamil.com

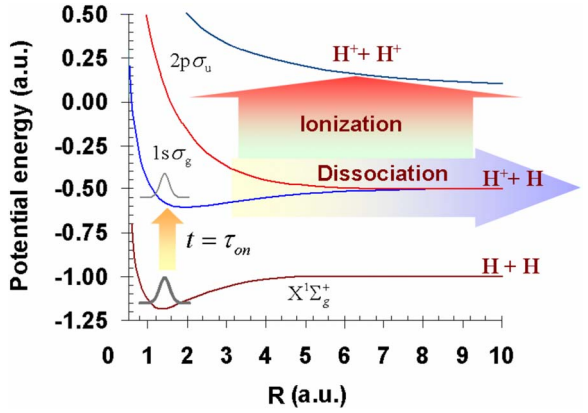

FIG. 1. (Color online) Sketch of the preparation and evaluation H_2^+ exposed to a linearly polarized intense femtosecond laser pulse. When the H_2 molecule is exposed to an intense laser pulse, the first electron is ejected at time t_{on} instantaneously. This process prepares a nuclear wave packet identical to the initial vibrational state of H_2 by a vertical Franck-Condon transition onto the H_2^+ ground σ_g state. During the remaining parts of the laser field envelope, complicated simultaneous dissociation-ionization processes of H_2^+ take place. Some parts of D_2^+ wave packet become unbound and outgoing through different channels, as $D+D^+$ through the dissociation channel (DC) and as D^++D^+ through the dissociation-ionization channel (DIC). The nuclear components in DIC possess both dissociation energy (DE) and Coulomb explosion energy (CEE).

$$f(t) = \exp\left[\frac{-2\ln(2)(t-t_{on})^2}{\tau_p^2}\right], \tag{4}$$

where τ_p is the full width at half maximum (FWHM) duration of the Gaussian shape of the pulse of the laser. The laser pulse in this simulation suddenly turns on at time t_{on}. We are assuming t_{on} is the time at which a H_2^+ (D_2^+) is suddenly created according a Frank-Condon transition from the natural H_2 (D_2) onto the H_2^+ (D_2^+) σ_g state (Fig. 1).

Now, for the time discretization of the TDSE—i.e., Eq. (2)—a propagator derived from split-operator methods has been used. This propagator is unitary and is obtained by combining the classical split operator and the Crank-Nicholson method [12–14].

The electronic dynamics is needed to the finest time step because its evaluation occurs on an attosecond time scale, but the time scale of nuclear dynamics is longer and then it is possible to apply a longer time step. Therefore, the time step is set to $\delta t_z = 0.02$ for the z and ρ components and $\delta t_R = 0.2$ for the R component.

The differential operators in Eq. (2) are discretized by 11-point difference formulas which have tenth-order accuracies [15]. More details of our calculations are described in our previous reports [11,15]. To solve the above TDSE numerically, we adopted a general nonlinear coordinate transformation for both electronic and nuclear coordinates. For spatial discretization, we have constructed a finite-difference scheme with a nonuniform (adaptive) grid for z and ρ electronic coordinates which are finest near the nuclei and coarsest at the border regions of the simulation box. A finite-difference scheme with an adaptive grid is used also for R coordinates that is finest for small R and becomes a coarse grid for large R. Use of a fine grid for electronic coordinates (z and ρ) near the nuclei and for small values of the nuclear distance coordinate (R) improves the treatment of the electron dynamics near the nuclei (the Coulomb singularities) and bound states of the nuclear dynamics, while use of a coarse grid near the borders improves the speed of calculations. The grid points for z, ρ, and R coordinates are 500, 500, and 500, respectively. The finest grid size values in this adaptive grid schemes are 0.13, 0.2, and 0.025 for, respectively, z, ρ, and R coordinates. The grids extend up to $z^{\max}=34$, $\rho^{\max}=25$, and $R^{\max}=16$.

In intense laser field, some parts of the D_2^+ wave packet become unbound and outgoing through different channels. A part of this unbound wave packet becomes outgoing as $D+D^+$ through a dissociation channel (DC) that is not concerned in this article and the other part becomes outgoing through a dissociation-ionization channel (DIC) as D^++D^+ (Fig. 1), which we study in this article. The nuclear components in this channel (DIC) possess both dissociation energy (DE) and Coulomb explosion energy (CEE).

The accurate kinetic spectra of different decay channels—i.e., ionization and dissociation or both simultaneously—can be determined by the virtual detector method [11,16]. The virtual detector method makes it possible to precisely define and distinguish outgoing norms and energy from different DC and DIC channels. This method allows us to accurately determine the CEE and DE of nuclear fragments through the DIC. More details about the virtual detectors method and its abilities are represented in our previous reports [11,17].

One of the main purposes of this work is a comparison between the present simulation results and the recent experimental results [5,6]. The amount of experimental research that has been started directly with H_2^+ and D_2^+ molecular ions are extremely few [18]. Most experiments have been performed using H_2 and D_2 molecules, and during the rise of the femtosecond laser pulse, H_2^+ (D_2^+) molecular ions are created. These pulses are usually focused to peak intensities of $\sim 10^{13}-10^{15}$ W/cm^2 into a gas jet of unaligned H_2 or D_2 neutral molecules. When a H_2 (D_2) molecule is exposed to a linearly polarized intense femtosecond laser pulse, the first electron is ejected during the rising laser pulse. We assume that the ejection of this first electron occurs at time t_{on} instantaneously via tunneling (Fig. 1). Also, we suppose that this process prepares a nuclear wave packet identical to the initial vibrational state of H_2 (D_2) via a vertical Franck-Condon transition onto the H_2^+ ground σ_g state as depicted in Fig. 1. In addition, we assume that at the time of the ejection of the first electron, the H_2 (D_2) molecule [and then H_2^+ (D_2^+)] is aligned with the linearly polarized intense femtosecond laser pulse. During the remaining parts of the laser field envelope, the complicated dissociation-ionization processes of H_2^+ (D_2^+) take place.

In this work, D_2^+ is exposed to femtosecond laser pulses with two different FWHM durations ($\tau_p=40$ and 140 fs). The intensities of these two femtosecond laser pulses are equal to 1.0×10^{14} W cm^{-2}, but their wavelengths are different and equal to 800 and 1200 nm, respectively. In these simulations, the femtosecond laser pulses turn on suddenly at two cycles before the peak of the laser pulse envelop and the simula-

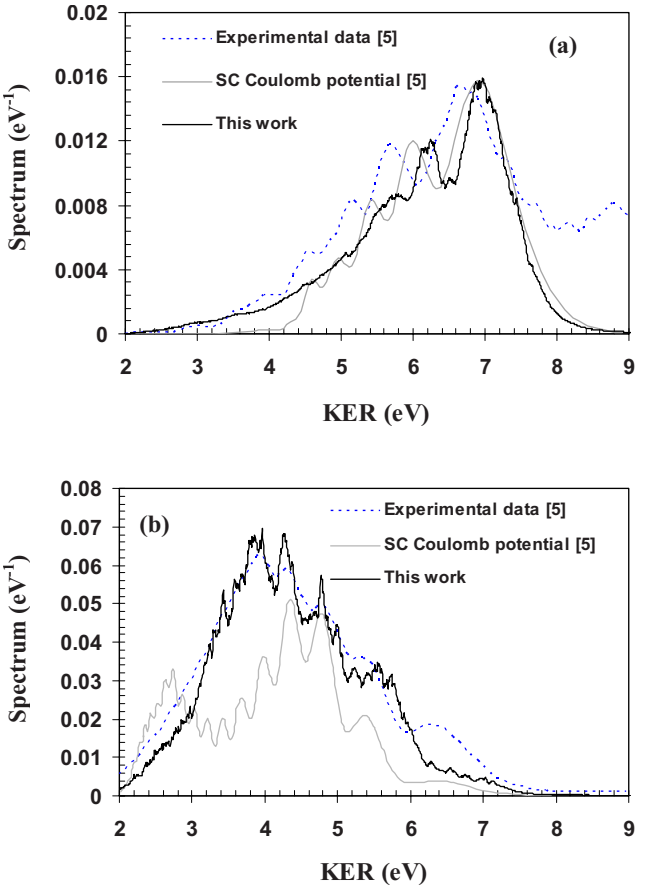

FIG. 2. (Color online) The kinetic energy release (KER) spectra of nuclear energy of D_2^+ exposed to femtosecond laser pulses with different FWHM durations and wavelengths: (a) τ_p=40 of I=1 $\times 10^{14}$ W/cm^2 intensity and λ=800 nm wavelength and (b) 140 fs of $I=1\times10^{14}$ W/cm^2 intensity and λ=1200 nm wavelength. The results of this work (black lines) are compared with the results of experimental research (dotted lines) [5,6] and the theoretical calculation with the SC potential approximation (gray lines) [5,6].

tions start just at this moment. The nuclear kinetic energy release (KER) relating to only the DIC for this molecular ion in these intense short laser pulses is showed in Fig. 2. The results of this simulation (black lines) are compared with the experimental results (dotted lines) [5,6] and theoretical calculation with the SC approximation (gray lines) [5,6]. In the experimental research [5,6], the gas jet of unaligned D_2 and H_2 is exposed to the femtosecond laser pulses. It is important to note that the uncertainty in the peak intensity in the experimental work [5,6] is about 10% at 800 nm and 30% at 1.2 μm and 1.4 μm wavelength and the uncertainty in the pulse duration is about $\pm$10%. It is surprising that in spite of the several assumptions considered in the setup of the simulation and the mentioned uncertainty involved in the experiment, there is good agreement between the KER of the experiment and simulation. There is an explicit difference between theoretical and experimental results in the high KER above ~7.6 eV in Fig. 2(a). This high KER in the experimental results seems to be related to the effect of nonaligned molecules [Fig. 16(c) of the Ref. [6]].

The KER of the DIC (D^++D^+) contains simultaneously both dissociation and ionization energies (DIEs); i.e., it possesses CEE ($1/R$) and DE. The signification of the DE in the KER spectra is often ignored. We recently predicted that the DE spectra are not sharp and ignorable and their structure can cause considerable changes in the structure of the KER spectra [19]. The simulation results for the DE and CEE spectra are depicted in Fig. 3 with blue and gray lines, respectively, and compared with the KER of the DIC (red lines) taken from Fig. 2. Figure 3 shows precisely that the DE spectra do not have a very sharp peak about a distinct value, but a relatively wide Gaussian shape distribution that shows peaks for Fig. 3(a) about ~1.6 eV and for Fig. 3(b) about ~0.3 eV. The overall shapes of the KER spectra resemble the CEE spectra. These figures show that it is possible to relate various parts of the KER and CEE spectra together. The numbers over graphs show these relations.

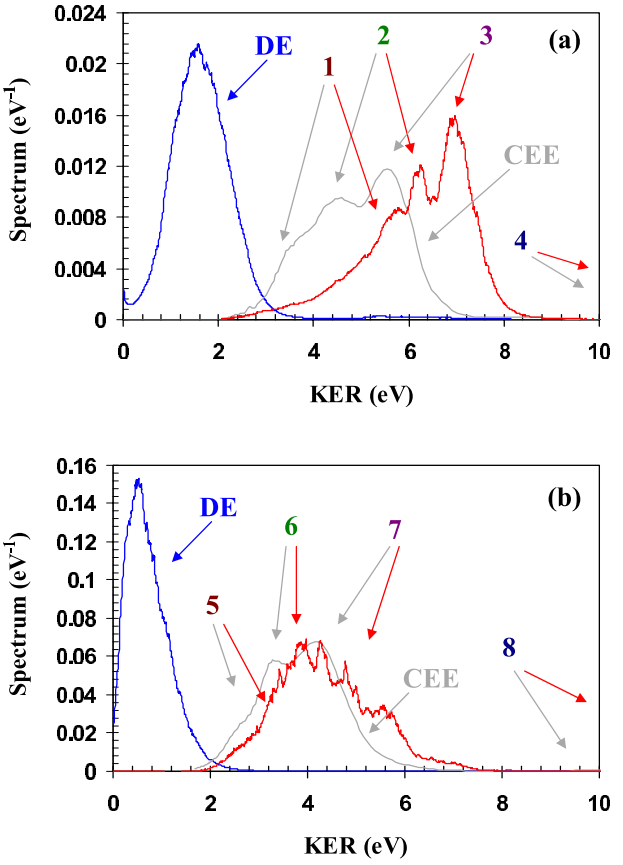

FIG. 3. (Color online) KER spectra (red lines) and their substructures the CEE (gray lines) and DE spectra (blue lines).

Figure 3 shows that the overall shape of the KER and CEE spectra are similar. The extent of modulation and displacement of KER with respect to CEE depends on the distribution of DE. The magnitude of the displacement of the peaks in Fig. 3(a) is about ~1.6—i.e., corresponding to the location of the peak of DE in Fig. 3(a). The average of the magnitude of the displacement in Fig. 3(b) is also about the location of the maximum of the DE spectrum—i.e., ~0.3 eV. Therefore, the magnitude of the displacement in Fig. 3(b) compared to Fig. 3(a) is small, but the structure of the KER with respect to CEE in Fig. 3(b) is more complicated than Fig. 3(a) and more peaks appear in the KER spectrum of Fig. 3(b) with respect to Fig. 3(a). Therefore, com-

parison of the spectra in Figs. 3(a) and 3(b) shows that altogether the DE in Fig. 3(b) has a sharper Gaussian shape distribution and results in smaller displacements in the KER spectrum in comparison with the CEE, but results in a more complicated structure for the KER with respect to CEE. The corresponding peaks of the KER and CE in Fig. 3(a) can be related easier than Fig. 3(b). The magnitude of the overall displacement of the KER spectra with respect to the CEE spectra helps us to determine these relations (the numbers on the graphs determine these relations).

An interesting and complicated phenomenon for H_2^+ in an intense laser field is the enhancement of the ionization rate as a function of internuclear separation, which results in maxima at some critical internuclear distances (R_C). This phenomenon has been shown theoretically, but with the BOA [19,20]. The H_2^+ molecular ion exhibits some critical distances (R_C) at which the molecular ionization rate exceeds the atomic rate by several orders of magnitude and proposes that the last electron is ejected mainly at much longer internuclear distances than the equilibrium internuclear separation. This effect has a special position in the interpretation of the molecular dynamics and fragmentation in an intense laser field [5,6,21] and Coulomb explosion imaging (CEI) [22]. Recently, precise calculations of the ionization rates based on the BOA have been developed [19,20,23].

It is surprising and important to investigate the (enhanced) ionization rate and critical distance beyond the BOA. It is clear that whenever R_C becomes longer, the CEE and then the total KER become smaller. When the electron of D_2^+ is ejected mostly at R_C, the two positive deuteron ions are exposed to simultaneously mutually repulsive force (Coulomb explosion). The magnitude of this repulsive force is proportional to the reciprocal of R_C. Therefore, it is predictable from the results of Fig. 2 that the R_C of Fig. 2(b) will be longer than Fig. 2(a). Figure 4 shows the R-dependent nuclear distributions of the DIC of D_2^+ which are, respectively, related to Figs. 2 and 3. Figure 4 represents the real enhanced ionization beyond the BOA. The R-dependent nuclear distributions and kinetic spectra in Figs. 2–4 have been derived by the virtual detector method [11,16]. The structure and variations of the KER in Fig. 2 can be related to the structure of the R-dependent non-BOA ionization rates in Fig. 4 as shown by numbers on the plots in Figs. 3 and 4. The plots in Fig. 4 show the R-dependent nonscaled ionization rates.

The CEE spectra in Fig. 3 have been extracted by using of the results of Fig. 4. The relation of the various parts of Fig. 4 and the CEE spectra in Fig. 3 has been determined with the depicted numbers. Figure 1 shows that the maximum amplitude of the nuclear distribution functions of H_2^+ created by the Frank-Condon transition from H_2 is about $R \sim 1.5$, but Fig. 4 shows that the ionization rate for the points about this nuclear distance (~ 1.5) is negligible. The maximum of the ionization rates is located for Fig. 4(a) at about ~ 4.4 and for Fig. 4(b) at about ~ 6. Figure 5 of Ref. [17] shows for $I=1 \times 10^{14}$ W/cm^2 intensity and $\lambda = 1064$ nm wavelength that R_c's appear at about ~ 6 and 9.5 for $\tau_1 = 0$ (the rising time of the laser pulse) and Fig. 1 of Ref. [11] shows for $I=1 \times 10^{14}$ W/cm^2 intensity and $\lambda = 790$ nm wavelength that R_c's are located at about ~ 5, 7, and 9.5. Comparison of the BOA and non-BOA shows that these parameters in the simulations in this work adjust to some values that result in EI to be strong only for small values of nuclear distance in the ionization signals. As we mentioned in a previous report [19], when the duration of ionization is short, the motion of nuclei is slow during the course of the ionization process and the system has little chance to evolve to large values of R during a passing laser pulse, and therefore, the ionization signal for larger values of R will be weak or even null. Therefore, the initial nuclear distribution and duration and intensities of the pulse laser are the effective parameters that determine the shape of the ionization signal. Comparison of the BOA and non-BOA shows that these parameters in the simulations in this work are such that the results in EI are strong only for small values of the nuclear distance in the ionization signals.

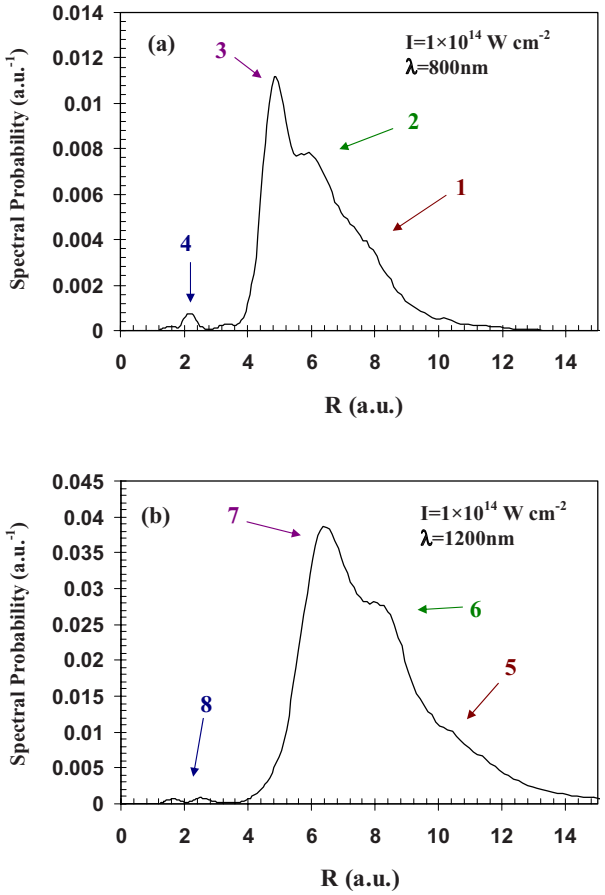

FIG. 4. (Color online) The nuclear R-dependent distribution of the ionization channel of D_2^+ for the two related simulations in Fig. 2, respectively.

CONCLUSION

In summary, it appears that the electronic full dimensional TDSE without any SC approximation can simulate very well recent experimental results and the Sc approximation can be successful in some cases and fails to simulate some experimental results. In simulations of one- and two-electron systems often the SC approximation is used. This work to some extent explores the validity and ability of this approximation

and the possibility of the application of the SC approximation to study and simplify such complicated systems.

The relation of the nuclear kinetic energy distributions of the DIC and the *R*-dependent ionization rate clearly was explored and thus the EI phenomenon was confirmed beyond the BOA. Therefore, on the basis of these simulations, we confirm directly the existence of the critical internuclear distance.

It was shown that in the KER structure, although the CEE substructure plays a fundamental role, the DE substructure resulting in the relative KER spectrum is modulated and displaced with respect to the CEE spectrum. Therefore, in a precise reconstruction of the vibrational nuclear wave function or wave packet from the total KER spectra of the DIC, an accurate determination of the structure of both the CEE and DIE spectra is necessary.

ACKNOWLEDGMENTS

I have benefited from valuable and stimulating discussions with Professor H. Sabzyan. The author would like to thank the University of Isfahan for financial support and research facilities and also the Isfahan High Performance Computing Center (IHPCC).

[1] M. Lein, J. Phys. B **40**, R135 (2007); M. Yu. Ivanov, A. Scrinzi, R. Kienberger, and D. M. Villeneuve, *ibid.* **39**, R1 (2006); T. Brabec and F. Krausz, Rev. Mod. Phys. **72**, 545 (2000); A. Giusti-Suzor, F. H. Mies, L. F. DiMauro, E. Charron, and B. Yang, J. Phys. B **28**, 309 (1995).

[2] A. Rudenko, V. L. B. de Jesus, Th. Ergler, K. Zrost, B. Feuerstein, C. D. Schröter, R. Moshammer, and J. Ullrich, Phys. Rev. Lett. **99**, 263003 (2007).

[3] Q. Su and J. H. Eberly, Phys. Rev. A **44**, 5997 (1991).

[4] B. Feuerstein and U. Thumm, Phys. Rev. A **67**, 043405 (2003).

[5] A. Staudte, D. Pavičić, S. Chelkowski, D. Zeidler, M. Meckel, H. Niikura, M. Schöffler, S. Schössler, B. Ulrich, P. P. Rajeev, Th. Weber, T. Jahnke, D. M. Villeneuve, A. D. Bandrauk, C. L. Cocke, P. B. Corkum, and R. Dörner, Phys. Rev. Lett. **98**, 073003 (2007).

[6] S. Chelkowski, A. D. Bandrauk, A. Staudte, and P. B. Corkum, Phys. Rev. A **76**, 013405 (2007).

[7] H. Ebadi and H. Sabzyan, J. Iran. Chem. Soc. (to be published).

[8] A. D. Bandrauk and H. Z. Lu, Phys. Rev. A **72**, 023408 (2005); S. Saugout, E. Charron, and C. Cornaggia, *ibid.* **77**, 023404 (2008).

[9] J. R. Hiskes, Phys. Rev. **122**, 1207 (1961).

[10] A. D. Bandrauk and H. Z. Lu, Phys. Rev. A **62**, 053406 (2000).

[11] M. Vafaee and H. Sabzyan, J. Phys. B **37**, 4143 (2004).

[12] C. Pozrikidis, *Numerical Computations in Science and Engineering* (Oxford University Press, Oxford, 1998).

[13] B. Forenberg, *A Practical Guide to Pseudospectral Methods* (Cambridge University Press, Cambridge, England, 1996).

[14] A. D. Bandrauk and H. Shen, J. Chem. Phys. **99**, 1185 (1993).

[15] M. Vafaee, H. Sabzyan, Z. Vafaee, and A. Katanforoush, e-print arXiv:physics/0509072.

[16] B. Feuerstein and U. Thumm, J. Phys. B **36**, 707 (2003).

[17] M. Vafaee, H. Sabzyan, Z. Vafaee, and A. Katanforoush, Phys. Rev. A **74**, 043416 (2006).

[18] D. Pavičić, A. Kiess, T. W. Hänsch, and H. Figger, Phys. Rev. Lett. **94**, 163002 (2005).

[19] H. Sabzyan and M. Vafaee, Phys. Rev. A **71**, 063404 (2005).

[20] T. Zuo and A. D. Bandrauk, Phys. Rev. A **52**, R2511 (1995).

[21] Th. Ergler, A. Rudenko, B. Feuerstein, K. Zrost, C. D. Schröter, R. Moshammer, and J. Ullrich, Phys. Rev. Lett. **95**, 093001 (2005).

[22] S. Chelkowski, P. B. Corkum, and A. D. Bandrauk, Phys. Rev. Lett. **82**, 3416 (1999); S. Chelkowski and A. D. Bandrauk, Phys. Rev. A **65**, 023403 (2002), C. R. Courtney and L. J. Frasinski, Phys. Lett. A **318**, 30 (2003).

[23] L.-Y. Peng, D. Dundas, J. F. McCann, K. T. Taylor, and I. D. Williams, J. Phys. B **36**, L295 (2003).